

PHYSICAL PROPERTIES AND STRUCTURAL STUDIES OF $\text{Se}_{100-x}\text{Sb}_x$

M.M. EL-ZAIDIA, A. EL-SHAFI, A.A. AMMAR and M. ABO-GHAZALA

Physics Department, Faculty of Science, Menoufia University, Shebin El-Koom (Egypt)

(Received 2 October 1986)

ABSTRACT

The DTA thermograms of the system $\text{Se}_{100-x}\text{Sb}_x$, where $x = 5, 10$ and 15 , were recorded at the heating rates $5, 10, 15, 20$ and $30^\circ \text{C min}^{-1}$. The glass transition temperature (T_g), and the crystallization temperature (T_{cp}) were found to be heating rate dependent, while the melting temperature (T_m) was not. Increasing antimony content in this system leads to decreasing T_g , T_{cp} and T_m . The apparent activation energy of crystallization was $15.99, 25.135$ and $29.705 \text{ kcal mol}^{-1}$ for the compositions $x = 5, 10$ and 15 , respectively. The X-ray diffraction charts show that the crystalline phases formed are Se, Sb and Se_3Sb_2 .

INTRODUCTION

The easy glass forming region of the system Ge–Sb–Se has been studied [1]. The tendency to form glass even upon slow cooling is only possible if the bonding arrangement of the atoms in the melt coincide with that of cooled glass [1]. The glass structure can be thought of as made up of units for which a chemical compound can be envisaged [2]. Thus the tetrahedral GeSe_2 and trigonal Se_3Sb_2 structural unit can be thought of as distributed in the glass among the other constituents [3]. The optical and electrical properties of this system have been reported [3–6]. The electrical properties of the binary system, Se–Sb have been studied [7]. In this system, even a small amount of antimony strongly affects the crystallization process [8].

The aim of this work is to report the transition temperatures, the glass forming tendency, the non-isothermal phase transformation, and the structure of the crystalline phases of the system $\text{Se}_{100-x}\text{Sb}_x$, where $x = 5, 10$ and 15 , using DTA and X-ray techniques.

EXPERIMENTAL TECHNIQUE

Amorphous bulk samples belonging to the system $\text{Se}_{100-x}\text{Sb}_x$ where $x = 5, 10$ and 15 , were prepared by the usual melt quench technique. The con-

stituents Se and Sb were weighed and sealed in an evacuated silica tube, which was then heated at 850°C for 8 h. During the melting process the tube was frequently agitated in order to intermix the constituents, to ensure homogenization of the melt. The melt was then quenched in cold water.

The differential thermal analysis thermograms were recorded using a Shimadzu DTA-30 analyser. A constant mass (0.05 g) of amorphous powder samples was used.

The X-ray diffraction pattern of the amorphous and annealed samples were recorded using a Shimadzu XD-3 diffractometer with a scanning velocity of $20/2\theta \text{ min}^{-1}$. The radiation source was a Cu foil ($\text{Cu } K\alpha = 1.5405 \text{ \AA}$) with a Ni filter.

RESULTS AND DISCUSSION

DTA results

The DTA thermograms of the amorphous system $\text{Se}_{100-x}\text{Sb}_x$, where $x = 5, 10$ and 15 , were recorded at the heating rates $5, 10, 15, 20$ and $30^\circ\text{C min}^{-1}$ (see Fig. 1). These thermograms are characterized by an endothermic peak corresponding to the glass transition temperature (T_g), one exothermic peak denoting the crystallization temperature range, its maximum corresponding to the crystallization temperature (T_{cp}), and one endothermic peak denoting the melting temperature range of the material, its minimum corresponding to the melting temperature (T_m). Values of the transition temperatures T_g , T_{cp} and T_m are listed in Table 1. The data in this table show that for any given material the glass transition temperature (T_g), and the crystallization temperature (T_{cp}) shift to higher values as the heating rate (ϕ), increases. The melting temperatures (T_m) fluctuate around a mean value as the heating rate changes. This may be due to the fact that the relaxation time of the melting process is small compared to the time allowed by the various heating rates. Consequently, one should not expect the heating rate to have a strong effect on the peak of melting. On the other hand the glass transition and the crystallization processes are known to be slow. Therefore one can expect the heating rate to have a relatively strong effect on T_g and T_{cp} .

The detection of a single value of T_g for each composition indicates that the prepared glasses are homogeneous. The glass forming ability (K_{gl}) of these glasses is given by the relation [9]

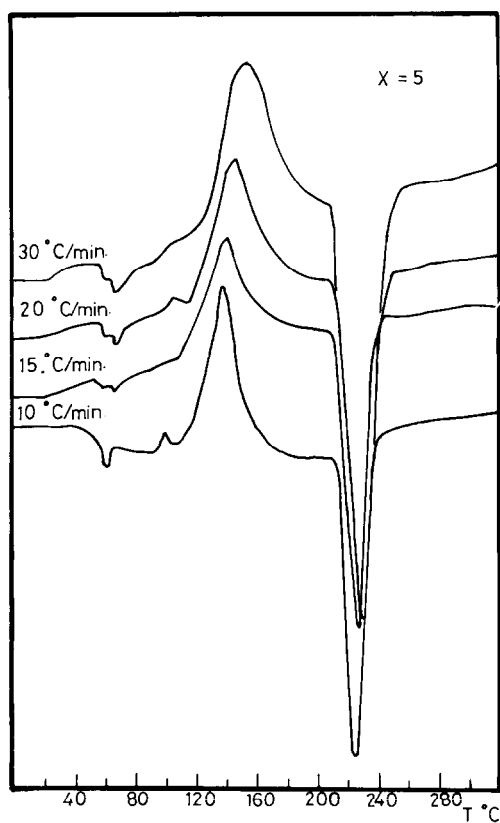
$$K_{gl} = (T_{cp} - T_g) / (T_m - T_{cp})$$

The use of such a formula is based on the assumption that all glasses are in a comparable state at T_g and that the glass forming tendency is directly proportional to the quantity $(T_{cp} - T_g)$, and inversely proportional to the quantity $(T_m - T_{cp})$. Table 1 shows that $(T_{cp} - T_g)$ increases, while $(T_m - T_{cp})$

TABLE 1

Transition temperatures

x	Rate ($^{\circ}\text{C min}^{-1}$)	Transition temperatures ($^{\circ}\text{C}$)			$(T_{\text{cp}} - T_{\text{g}})$ ($^{\circ}\text{C}$)	$(T_{\text{m}} - T_{\text{cp}})$ ($^{\circ}\text{C}$)	K_{gl}
		T_{g}	T_{cp}	T_{m}			
5	10	61.5	137	226	75.5	89	0.85
	15	66.0	141.5	229	75.5	87.5	0.86
	20	67.5	146.5	232	79.5	84	0.95
	30	67.5	154.0	230	86.0	76	1.13
10	5	51.5	126	224	74.5	98	0.76
	10	47.5	136	228	88.5	92	0.96
	15	54	140	225	86.0	85	1.01
	20	55.5	146	228.5	90.5	82	1.10
	30	56.0	153	225	97.0	72	1.35
15	5	52	123	226	71	103	0.69
	10	51	132	227	81	95	0.85
	15	53.5	136	224.5	84	87	0.97
	20	54.5	142	226	87.5	84	1.04
	30	56	150	224.5	94.0	75	1.25

Fig. 1. DTA thermograms of $\text{Se}_{100-x}\text{Sb}_x$, $x = 5, 10$ and 15 .

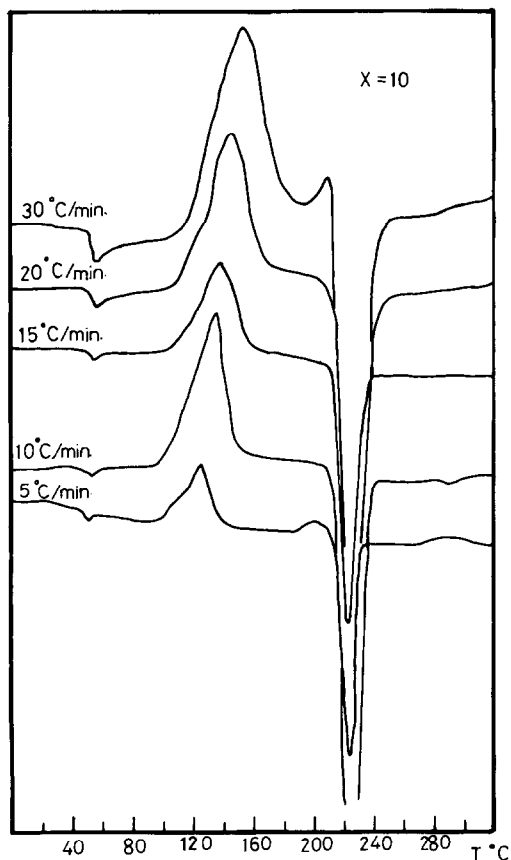


Fig. 1 (continued).

decreases as the heating rate increases. This result may indicate that the glass forming ability is heating rate dependent. This result is in a good agreement with previous data [10,11]. The phase diagram [8] of the binary system Se—Sb also confirms this result.

The transition temperatures T_g , T_{cp} and T_m of pure selenium were 60, 162 and 240 °C at the heating rate 3 °C min⁻¹ [12]. The addition of antimony to pure selenium causes a decrease of these transition temperatures. This may be attributed to the weak Sb—Sb and Se—Sb bond strengths compared to Se—Se [3].

The DTA thermograms have been used to study the amorphous—crystal-line transformation. This has been done by deducing the order of reaction (n) and the apparent activation energy of crystallization (E_c). The values of n were determined using the shape index method [13]. Table 2 shows that the values of n decrease on increasing either the heating rate or the antimony content. This may indicate that the process of amorphous—crystal-line transformation becomes undimensional on increasing the antimony

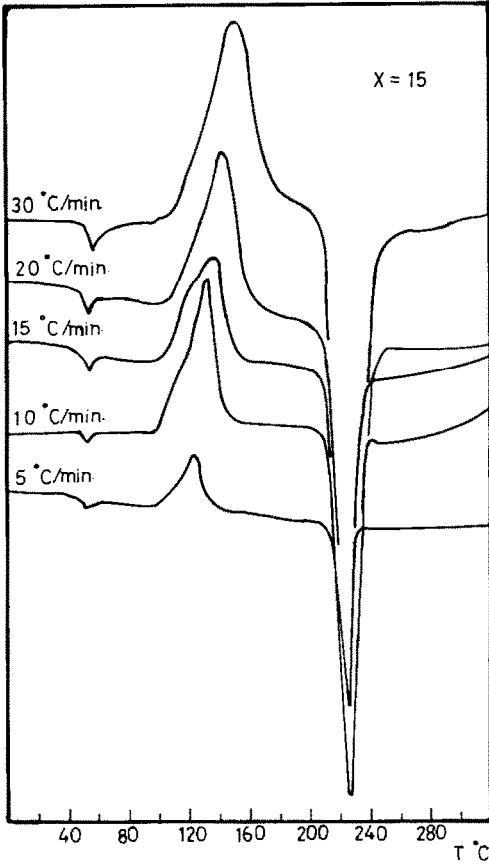


Fig. 1 (continued).

content. The values of (E_c) have been determined using the following equation [13,14]

$$\ln(T_{cp}^2/\phi) = \text{constant} - E_c/RT_{cp}$$

$$\ln \phi = \text{constant} + E_c/RT_{cp}$$

where R is the universal gas constant. The relations $\ln(T_{cp}^2/\phi)$ versus $(1/T_{cp})$ and $\ln \phi$ versus $(1/T_{cp})$ yield the values of E_c). Table 2 illustrates that the value of E_c increases as the Sb content increases. This may be due to a slowing down of the reconstruction process as the antimony atoms are precipitated in the selenium polymeric chains.

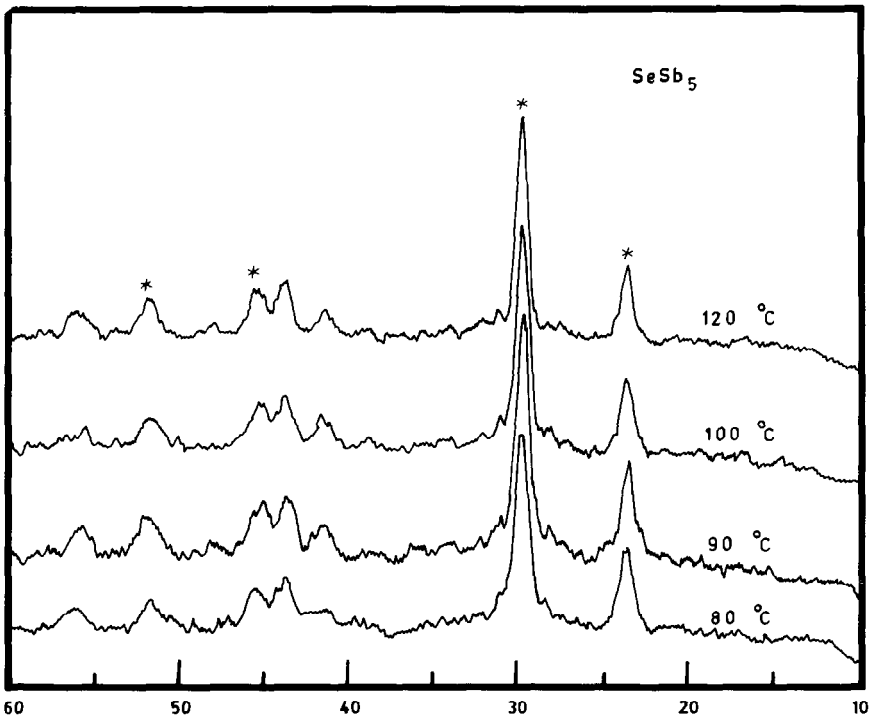
X-ray results

Figure 2 shows the X-ray charts for the three compositions $x = 5, 10$ and 15 . The samples were annealed at $80, 90, 100, 110$ and 120°C for a constant

TABLE 2

Values of n and E_c with respect to antimony content, x

x	Rate ($^{\circ}\text{C min}^{-1}$)	n	E_c (kcal mol $^{-1}$)	
			Kissinger	Ozawa
5	10	1.47	15.99	20.57
	15	1.42		
	20	1.40		
	30	1.37		
10	5	1.30	25.14	22.85
	10	1.17		
	15	1.13		
	20	1.11		
	30	1.06		
15	5	—	29.71	29.70
	10	1.13		
	15	1.10		
	20	1.08		
	30	1.03		

Fig. 2. X-ray diffraction pattern of $\text{Se}_{100-x}\text{Sb}_x$.

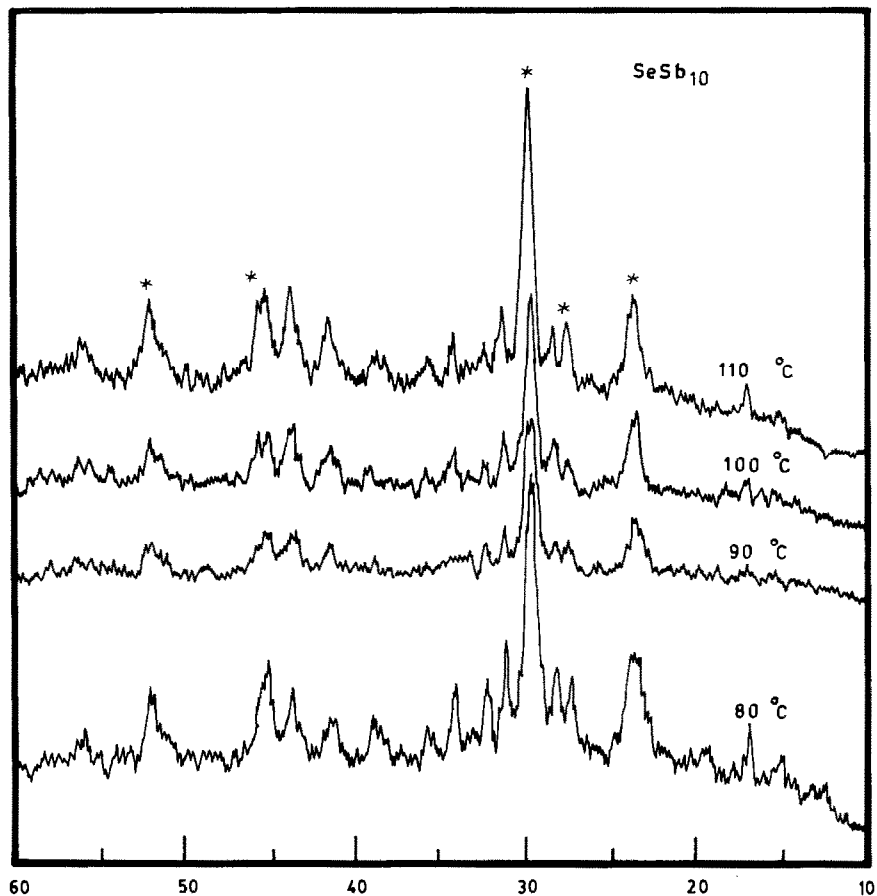


Fig. 2 (continued).

time (1 h), before testing. The annealing process leads to the creation of the same crystalline phases in all samples (Table 3) but with different concentrations. However, for all samples the intensities of the X-ray diffraction peaks were observed to increase as the annealing temperature increased. The peaks denoted by a star, in Fig. 2 will be used as references in analysing the X-ray data. The areas under the various peaks were plotted as a function of the annealing temperature for all compositions (Fig. 3). These results show that the growth of all crystalline phases is exponential. This may indicate that the process of growth is not simply due to the formation of bridges between Se and Sb atoms. This in turn, confirms the fact that the energy of crystallization, E_c , increases as the Sb content increases. The growth of the area under the peak in Fig. 3 shows that the crystalline Se phase was fast in all compositions, while this growth was slow in the case of crystalline Sb and Se_3Sb_2 phases. This means that the main crystalline phase is Se. This fact

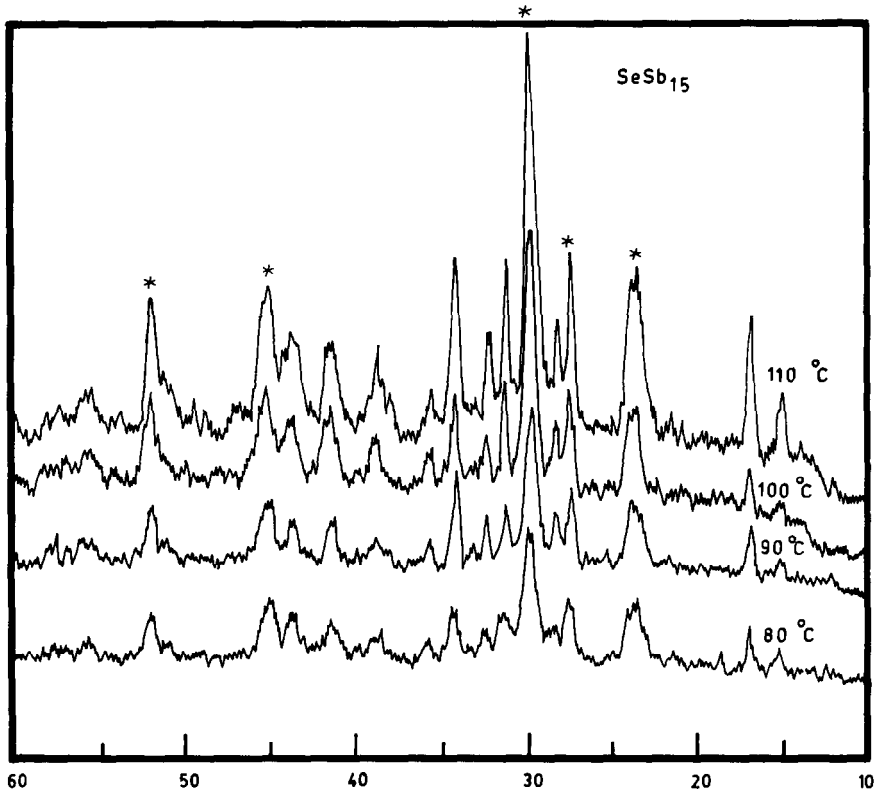


Fig. 2 (continued).

TABLE 3

X-ray crystallographic data

x	Crystal phase	2θ	d (Å)		(hkl)	Crystal form
			Exp.	ASTM		
5	Se	29, 30	3.666	3.670	$(3\bar{1}2)$	Hexagonal
		45	1.975	1.975	$(6\bar{6}2)$	
	Sb	24	3.753	3.753	(003)	Trigonal
		Se_3Sb_2	52	1.760	1.761	(061)
		56	1.646	1.646	(142)	
10	Se	29, 30	2.995	3.00	$(3\bar{1}2)$	Hexagonal
		45	2.071	2.071	-	
	Sb	24	3.751	3.752	(003)	Trigonal
		Se_3Sb_2	28	3.240	3.250	(100)
			56	1.641	1.646	(710)
15	Se	29, 30	2.985	3.00	(312)	Hexagonal
		45	2.000	1.996	-	
	Sb	24	3.750	3.750	(003)	Trigonal
		Se_3Sb_2	28	3.24	3.25	(100)
			56	1.754	1.754	(142)

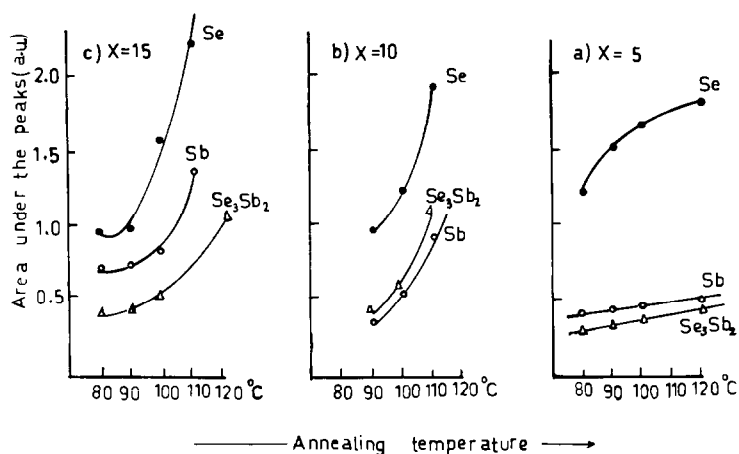


Fig. 3. Area under the peaks vs. annealing temperature.

has been confirmed by the occurrence of T_{cp} values for all compositions around that of pure Se from DTA results. This also has been confirmed by the detected melting temperature, T_m , which is very close to that of pure Se.

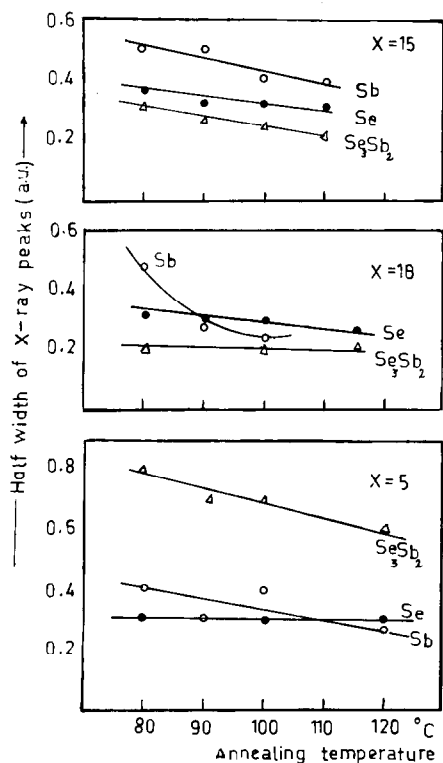


Fig. 4. Halfwidth of X-ray vs. annealing temperature.

The presence of the crystalline Se_3Sb_2 and Sb as minor phases may be confirmed since the eutectic point of SeSb crystalline phases is near 250°C .

Figure 4 shows the half width of the selected peaks as a function of annealing temperature. The decrease in the halfwidth as the annealing temperature increases may indicate that some phase separation may occur. This observation is more pronounced in the case of $x = 15$ than the other two compositions. This fact leads to the limitation of the mode of reaction (n), which decreases as the Sb content increases.

REFERENCES

- 1 R.J. Patterson and M.J. Brau, Presented at the Electrochemical Society Meeting, May 1966, Cleveland, OH.
- 2 H. Fritsche in J. Tauc (Ed.), *Amorphous and Liquid Semiconductors*, Plenum, London, 1974, p. 221.
- 3 A. Giridhar, P.S.L. Narsimham and S. Mahdevan, *J. Non-Cryst. Solids*, 37 (1980) 165.
- 4 J.A. Savage, P.J. Webber and A. Mpitt, *J. Mater. Sci.*, 13 (1978) 859.
- 5 M.R. Rehtin, A.R. Hilton and D.J. Hayes, *J. Electron. Mater.*, 4 (1975) 347.
- 6 A.R. Hilton and D.J. Hayes, *J. Non-Cryst. Solids*, 17 (1975) 319.
- 7 M.M. El-Zaidia, A.A. Ammar, A. El-Shafi and M. Abo-Ghazala, *J. Fac. Educ. Ain Shams Univ., Egypt* (1986) in press.
- 8 H. Krebs, *Angew. Chem. Int. Ed. Engl.*, (1966) 544.
- 9 P.I.K. Onorato and D.R. Hopper, *J. Non-Cryst. Solids*, 41 (1980) 189.
- 10 D.D. Thornburg, *Mater. Res. Bull.*, 9 (1974) 1481.
- 11 M. Lasocká, *J. Mater. Sci.*, 11 (1976) 1771.
- 12 H.P.D. Lanyon and E.F. Hockings, *Phys. Status Solidi*, 17 (1966) K.
- 13 H.E. Kissinger, *Anal. Chem.*, 29 (1957) 1702.
- 14 T. Ozaw, *J. Therm. Anal.*, 2 (1970) 301.